A Two-State Packet Error Model for Vehicle-to-Infrastructure Communications

Veronika Shivaldova and Christoph F. Mecklenbräuker

Institute of Telecommunications, Vienna University of Technology
Gusshausstrasse 25/389, 1040 Vienna, Austria
email: {veronika.shivaldova, cfm}@tuwien.ac.at

***Abstract*—In this paper we propose and analyze a novel, computationally inexpensive packet-error model for infrastructure-to-vehicle (I2V) communications. Based on real-world measurements using IEEE 802.11p devices, the proposed model incorporates the physical layer characteristics and propagation effects in an authentic highway environment with real vehicular traffic. With only a small set of parameters, the model allows to simulate time series of packet error events with a Hidden Markov Model (HMM). We propose this packet error model for the simulation of vehicular connectivity in the context of intelligent transport systems.**

I. Introduction

Simulation became an important development tool for majority of communication systems, including vehicular communications. While hardware part of the transmission chain can be efficiently reproduced by simulator according to corresponding standard, modeling of wireless media between the transmitter and the receiver turns out to be quite a challenging problem. Results of real-world measurements show that deterministic radio propagation models typically assuming exponential path loss and omnidirectional signal propagation should be avoided, since they do not capture such significant realistic effects as small scale fading and shadowing. These effects considerably influence transmission range and packet error rates of vehicular communication systems, especially on intersections [1], [2]. Measurement results in [3] show that the number of available propagation paths increases dramatically when vehicle approaches an intersection and both the coverage and the throughput are strongly dependent on the number and the location of large scatterers. As has been shown by authors of [4] not only large scatterers as buildings, but also traffic signs can severely influence signal propagation properties by adding a constant delay and zero Doppler paths over time. Therefore realistic vehicular channel models, which are capable of capturing effects like small scale fading and shadowing, are crucial for improving the quality of simulations.

Two most common methods to reliably reproduce realistic vehicular channels are replay models and ray-tracing models. For replay models the transmission between real vehicles is observed in a city or highway environment and the resulting trace is directly used as an input for simulator [5], [6]. However despite of extremely high costs for performing such experiments, the obtained models are constrained to represent specific environment, namely the one where the measurements were taken. Ray-tracing models serving as an excellent approximation of the real-world measurements are more general [7], [8]. Here, propagation effects extracted from the real-world observations are used to analytically model vehicular channels. However, computational complexity of the ray-tracing models is fairly high and the resulting precision is not always necessary, e.g., in case of network simulators.

In most existing network simulators, physical layers is abstracted and extremely simplified, thereby ignoring realistic channel effects [9]. In order to provide accurate representation of physical layer and yet keep computational effort within a manageable dimension, stochastic models describing the wireless channel characteristics from a macroscopic point of view can be used.

In this paper we present a novel, computationally inexpensive packet-error modeling approach for infrastructure-to-vehicle (I2V) communications. The proposed model incorporates realistic physical layer characteristics, such as standard-compliant transmitter and receiver equipment, vehicle velocity, as well as authentic highway environment and traffic conditions. We introduce an elegant way to accurately reproduce measured I2V traces by a Hidden Markov Model (HMM) with only two states. Given a limited set of parameters, realistic packet error traces can easily be produced to replace the unreliable physical layer abstractions of existing simulation tools. In spite of simplified representation, this modeling approach is well suited for performance evaluation of higher layer protocols and applications such as, retransmission mechanisms and disruption tolerance for end-to-end connections.

II. Measurement Environment and Equipment

In order to establish the real world reference data for modeling the packet error behavior of I2V systems, we have conducted an extensive series of measurements on the highway A4 in Austria. Measurements were performed at a center frequency of 5.9 GHz with real vehicular traffic. Packets were transmitted with data rate of 6 Mbit/s and packet length of 500 Byte, default parameters of the PHY/MAC implementation based on ETSI ITS-G5A. For constant vehicle speed of

80 km/h (22.2 m/s), packet detection events were observed on the wireless media with rate of 153 Hz, i.e., one detection event each 6.53 ms or 0.1475 m.

The stretch of highway selected for the measurement is nearly straight and consists of three lanes. It is located in the industrial area connecting the city of Vienna with the international airport of Vienna. This fact implies three important characteristics of the measurement environment: considerably dense traffic, significant number of road signs and little vegetation. In order to increase influence of scattering objects, we have chosen a part of highway surrounded by a noise protection wall on one side.

As a roadside unit (RSU) transmitter we used an IEEE 802.11p standard compliant transceiver, provided by Kapsch TrafficCom. It consists of two directional antennas, an embedded computer with Ethernet connection for remote controlling, a global positioning system (GPS) receiver needed for synchronization and protection units. The radio front-end of the IEEE 802.11p transceiver was connected via a power splitter to two identical directional antennas. The transmitter antennas with gain of 14 dBi resulting in an equivalent isotropically radiated power of approximately 12.2 dBm were vertically polarized. The horizontal and vertical 3 dB antenna beamwidth are 30° and 40°, respectively. The antennas were mounted on the side of highway gantry (location coordinates 48.1474, 16.4994), 7.1 m above the road and were pointing in both directions of the highway, such that all lanes in all directions were homogeneously covered.

As an on-board unit (OBU) receiver we used the cooperative vehicle-infrastructure systems (CVIS) platform [10]. The CVIS platform is equipped with a CVIS communication architecture for land mobiles (CALM) M5 radio module implementing the IEEE 802.11p protocol and a GPS receiver, which constantly logs the exact position of the device. The OBU receiver was connected to the OBU antenna, mounted with magnets on the roof of the test vehicle (a "Ford Galaxy") at the height of approximately 1.7 m. As OBU antenna a wideband (1.7 - 6.0 GHz) surface mount antenna with ground plane independent omnidirectional radiation pattern, manufactured by "Mobile Mark" was used. The antenna performance is 5 dBi (peak gain) resulting in EIRP of 8.7 dBm.

While the RSU was transmitting constantly in broadcast mode, the OBU was recording only within the expected coverage range, i.e., approximately 500 m before and after passing the RSU location. For each detected event the OBU records time and location, as well as received signal strength. All detected events undergo a cyclic redundancy check (CRC), to determine whether the detected packet was correctly decoded or not. Based on the result of the CRC a binary error pattern of the measurement is created. We have to account for the case, that not all detected events were caused by actually transmitted packets and not all transmitted packets were detected by the receiver. Therefore, the binary error pattern created by the OBU was reexamined and completed in the post-processing stage. The error pattern overhaul procedure is based on the comparison of the unique packet identifier contained in the header of each decoded packet with that stored in the transmitter log-file.

III. Modeling Approach

For modeling an error pattern of I2V channel we propose to use a simple model introduced by Gilbert [11]. Gilbert model is a first-order two-state Markov model with one 'Good" and one "Bad" state, as shown in Fig. 1. Errors occur only in the Bad state and even then not always, but with probability $P_E > 0$. After an observation digit is produced according to the error probability of the current state a state transition takes place. Thus, the current digit of the error pattern is independent of the previous. The state transition is described by the probabilities of changing from the Good state to the Bad (P_{GB}) and from the Bad state to the Good (P_{BG}). Both states are persistent, i.e., $P_{GB} \ll 1 - P_{GB}$ and $P_{BG} \ll 1 - P_{BG}$, therefore the produced error pattern has bursty structure. Gilbert model is a HMM, since the current state of the model cannot be determined from neither the modeled nor the measured sequences and the model parameters $\lambda = \{P_{GB},\ P_{BG},\ P_E\}$ are not directly observable from training data.

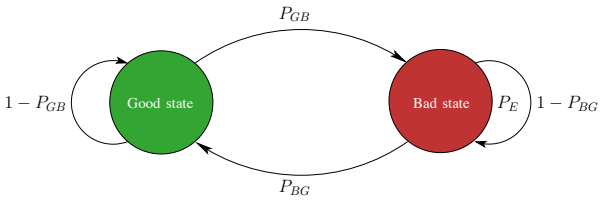

Fig. 1: Schematic illustration of Gilbert model.

Since the performance of the I2V link is strongly distance and environment dependent and varies significantly even within one measurement, it is impossible to accurately describe the whole error pattern with a simple model having just two states. Therefore in order to reproduce the measured error pattern we propose to divide it into N fractions corresponding to N non-overlapping distance intervals each of length ξ, referred as a granularity in the reminder of this paper. Transition and emission probabilities are estimated separately for each interval with the Baum-Welch estimation algorithm [12]. For the sake of estimating the probabilities, for each digit $k \in \{1, \dots K\}$ of the error pattern fraction from current interval n we calculate:

- forward probabilities, i.e., the probability of ending up in a particular state $\mathcal{S}$ given the first k observations in the sequence and the model λ, and
- backward probabilities, i.e., probabilities of observing the remaining $K - k$ digits of the error pattern given any starting point k and the model.

Forward probabilities α_{ij} are calculated as the ratio of the expected number of transitions from state $\mathcal{S}_i$ to state $\mathcal{S}_j$, divided by the expected time spent in the state $\mathcal{S}_i$. Backward probabilities β_i are calculated as the ratio of the expected time spent in the state $\mathcal{S}_i$ and observing symbol $\mathcal{O}$ divided by the expected number of times spent in state $\mathcal{S}_i$. Based on

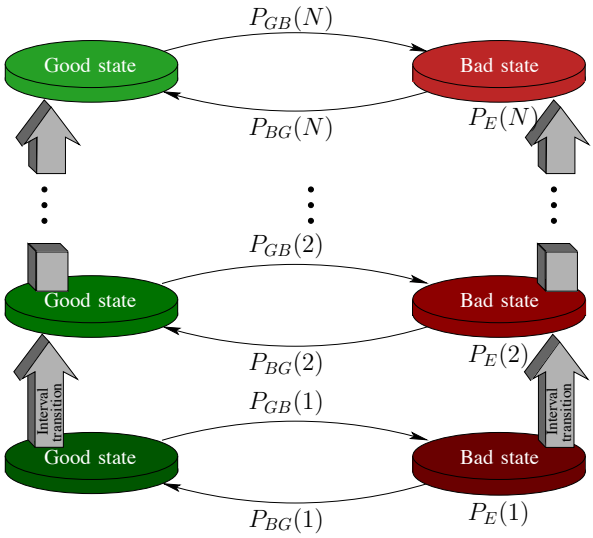

Fig. 2: Schematic illustration of range-dependent modified Gilbert model.

the forward and backward probabilities initial set of model parameters $\lambda = \{P_{GB},\ P_{BG},\ P_E\}$ is re-estimated. It has been proven that either initial model λ defines the critical point of likelihood function, in which case it is the same as re-estimated model ($\lambda = \bar{\lambda}$), or observation sequence is more likely to be obtained from the re-estimated model $\bar{\lambda}$. The forward-backward procedure is iteratively repeated until the desired tolerance of testing convergence is achieved.

Since the Baum-Welch algorithm finds only a local maximum, it is sensitive to the choice of initial set of parameters λ. To allow for accurate and fast parameter estimation, the initial set of probabilities was defined based on the matching of experimentally obtained error-free fraction length distribution, as proposed in [11]. Since the events leading to decoding errors on the receiver side are not related to one another, the time spent between such events and the length of error-free fractions has geometric distribution [13]. As can be seen from Fig. 3(a) the length of error-free fractions of the measured error pattern is indeed very close to geometric distribution, which further verifies the validity of our modeling approach.

Once the model parameters for all N intervals are estimated, we can combine them as shown in Fig. 2 to form a range-dependent modified Gilbert model able to reproduce error pattern of the whole measurement. The initial state of this model for the first interval is chosen randomly according to the measured initial state distribution. While for all subsequent intervals the initial state is the same as the final state of the previous interval, i.e., the model remains in the same state during the interval transition. The interval transition and thus change of the transition and emission probabilities ($P_{GB},\ P_{BG},\ P_E$) occurs when the vehicle leaves the range of current interval.

IV. Results

Choice of granularity is essential for parameter estimation accuracy of the range-dependent modified Gilbert model. On one hand, granularity cannot be chosen arbitrary small, since by dividing the error pattern into shorter fractions we might break long runs in one of the states apart, influencing by that the transition probabilities. The shorter the interval length is, the more often we have to disrupt the original error sequence, until we eventually end up with very short fractions consisting of all the same digits (either 1 or 0). In this case probability of transition from one state to the other will tend to zero. On the other hand, estimating set of model parameters for large intervals would lead to performance averaging over a large distance and therefore it wouldn't be possible to capture and reproduce any location dependent propagation channel effects as, e.g., small scale fading and shadowing.

In order to define the range of granularities for modeling, we have first analyzed the influence of breaking the measured error pattern into equally large intervals with different granularity. The analysis was based on the gap and the burst lengths distribution. The gap length is the number of subsequently received error-free packets, while the number of subsequently received erroneous packets is called the burst length. The green solid line in Fig. 3 shows empirical cumulative density function (CDF) of the gap (left) and the burst (right) lengths of the original measurement. The curve represents an average over 10 repetitions of the same measurement. Dividing original measurement into equally large intervals has shown that the gap and the burst length distribution remained unchanged for interval size $\xi \geq 30\,\mathrm{m}$. While the gap and the burst length distributions of the measurements divided into intervals with $\xi < 30\,\mathrm{m}$ deferred from the distribution of the original error pattern significantly. This difference can be observed the best when comparing the green and the magenta solid lines in Fig. 3. Here, the magenta curves represent distribution of the measured error pattern divided into intervals of length $\xi = 10\,\mathrm{m}$.

Therefore, the model parameters were estimated with 78 different granularities in the range $\xi \in \{30\,\mathrm{m}, 40\,\mathrm{m}, \ldots, 800\,\mathrm{m}\}$, where for model parameter estimation with $\xi = 800\,\mathrm{m}$ measured error pattern was used as the whole. The empirical CDFs of the gap and the burst lengths, obtained as an average over 10.000 realizations of the range-dependent modified Gilbert model with granularity $\xi = 30\,\mathrm{m}$ and $\xi = 800\,\mathrm{m}$ are shown in Fig. 3 with red and blue, respectively. We observe that the statistical distributions of the modeled sequences provide close approximation of the measurement for both the smallest and the largest granularities.

To further visualize the model accuracy we calculate the frame success ratio (FSR), a metric often used to characterize the performance of the vehicular radio link. The FSR is defined as the number of error-free packets divided by the total number of detection events, during the time interval $T = \Delta d/v$. Here, v is the velocity of the test vehicle and we set $\Delta d = 10\,\mathrm{m}$, resulting in $T = 0.45\,\mathrm{s}$ for a vehicle velocity of 80 km/h. Fig. 4

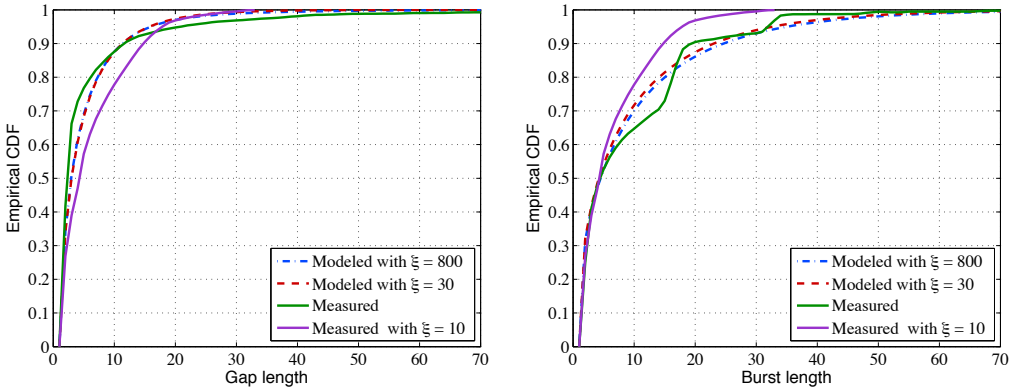

(a) Empirical CDF of gap length distribution.

(b) Empirical CDF of burst length distribution.

Fig. 3: Comparison of empirical CDFs of gap and burst lengths obtained from measured and modeled error patterns.

shows FSR performance of a randomly chosen measured error pattern in green and that of error patterns generated with the model for granularity $\xi = 30\,\mathrm{m}$ and $\xi = 800\,\mathrm{m}$ in red and blue, respectively. Here FSR curves are plotted versus the distance d, where the origin of the abscissa ($d = 0\,\mathrm{m}$) corresponds to the position of the RSU. Negative values on the abscissa correspond to locations where the vehicle was approaching the RSU and positive distances represent the vehicle locations after passing the RSU.

In addition we specify a set of main performance indicators, such as throughput, error fraction and coverage range in order to perform qualitative comparison of the measured and the modeled sequences. In this context, the throughput is defined as a number of packets successfully decoded during one measurement multiplied by the packet length. The error fraction is a percentage of erroneously decoded packets during one measurement. While for coverage range analysis we introduce the reliable communication range (RCR) and the unreliable communication range (UCR), as in [14]. The RCR is the absolute distance from the RSU, within which the obtained FSR values are greater than 0.7 and the UCR is the distance at which the FSR drops below 0.1 for the first time. Therefore, the RCR represents the range over which high quality communications can be established and for RCR $\leq |d| \leq$ UCR we can not reliably guarantee any communication quality.

Comparison of the main performance indicators for the modeled and the measured error patterns is shown in Table I. It can be seen that the throughput, the error fraction and the UCR can be quite accurately reproduced by the model with both the smallest and the largest granularities. While with respect to the RCR, model with smaller granularity fits the measurements much better. The RCR of the model with granularity $\xi = 800\,\mathrm{m}$ is on average $36\,\%$ less than that of the measurement, while the difference between measured and modeled with granularity $\xi = 30\,\mathrm{m}$ RCR is just $3\,\%$. This fact becomes even more evident, when comparing the FSR curves in Fig. 4. While the red FSR curve reproduces precisely the majority of measured propagation channel effects, the blue curve, parameters of which were estimated over the whole measurement shows rather the average FSR behavior, ignoring by that realistic location dependence. This can be observed the best at $d = 0(\pm 10)\,\mathrm{m}$, where the test vehicle is passing directly under the RSU. Due to the fact that the signal strength radiated by a set of directional antennas is rather weak directly below the gantry, we observe a drop of the FSR that is well reproduced by the model with granularity $\xi = 30\,\mathrm{m}$, but not with granularity $\xi = 800\,\mathrm{m}$. Furthermore, models with smaller granularities can better reproduce error patterns measured on the edges of the coverage range, where the FSR curve fluctuates much stronger.

The above considerations clearly state that the granularity of the proposed model should be chosen as a trade-off between the accuracy of representation and the number of model parameters and is strictly application dependent. Since we do not aim to exactly reproduce the specific measurement environment, but rather present a general I2V model, in context of this paper we provide model parameters estimated for granularity $\xi = 100\,\mathrm{m}$. Transition and emission probabilities with corresponding $95\,\%$ confidence intervals for the range-dependent modified Gilbert model with granularity of $\xi = 100\,\mathrm{m}$ are summarized in Table II. The $95\,\%$ confidence intervals were calculated based on 10.000 model realizations. Analyzing the probabilities, we conclude that the dependence of the model parameters on the distance is nearly symmetric around the location of the RSU. The change of model parameters according to the distance between the RSU and the OBU is quite intuitive. The probabilities of staying in the Good state and changing from the Bad state to the Good state are increasing, while the error probability is decreasing with decreasing distance between the OBU and the RSU. Slightly larger probabilities $\hat{P}_{GB}$ and $\hat{P}_E$, as well as slightly smaller $\hat{P}_{BG}$ in the interval $-50 \leq d \leq 50\,\mathrm{m}$ represent the drop of the FSR curve in the closest vicinity of the RSU (cf. green curve in Fig. 4), which was obtained due to specific choice and positioning of the RSU equipment.

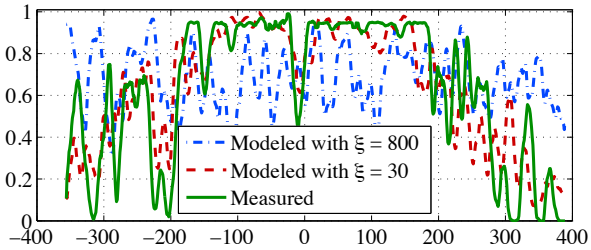

	Modeled ξ = 800 m	Modeled ξ = 30 m	Measured
Throughput [Mbit]	1.72	1.68	1.60
Error fraction [%]	33	31.8	31.3
RCR [m]	98	150	153
UCR [m]	380	375	370

Fig. 4 & TABLE I: Comparison of FSR curves and main performance indicators for measured and modeled error patterns.

TABLE II: Estimated parameters of the range-dependent modified Gilbert model with $\xi = 100\,\mathrm{m}$.

Distance range	$\hat{\mathbf{P}}^{-}_{\mathbf{GB}} \leq \hat{\mathbf{P}}_{\mathbf{GB}} \leq \hat{\mathbf{P}}^{+}_{\mathbf{GB}}$	$\hat{\mathbf{P}}^{-}_{\mathbf{BG}} \leq \hat{\mathbf{P}}_{\mathbf{BG}} \leq \hat{\mathbf{P}}^{+}_{\mathbf{BG}}$	$\hat{\mathbf{P}}^{-}_{\mathbf{E}} \leq \hat{\mathbf{P}}_{\mathbf{E}} \leq \hat{\mathbf{P}}^{+}_{\mathbf{E}}$
-450:-350	$0.220 \leq 0.280 \leq 0.350$	$0.014 \leq 0.023 \leq 0.093$	$0.855 \leq 0.929 \leq 0.987$
-350:-250	$0.108 \leq 0.130 \leq 0.154$	$0.066 \leq 0.099 \leq 0.138$	$0.883 \leq 0.923 \leq 0.961$
-250:-150	$0.067 \leq 0.080 \leq 0.095$	$0.101 \leq 0.143 \leq 0.195$	$0.915 \leq 0.956 \leq 0.992$
-150:-50	$0.064 \leq 0.073 \leq 0.090$	$0.302 \leq 0.521 \leq 0.721$	$0.682 \leq 0.747 \leq 0.781$
-50:50	$0.070 \leq 0.085 \leq 0.097$	$0.096 \leq 0.260 \leq 0.405$	$0.473 \leq 0.636 \leq 0.816$
50:150	$0.023 \leq 0.062 \leq 0.069$	$0.080 \leq 0.541 \leq 0.644$	$0.702 \leq 0.791 \leq 0.869$
150:250	$0.072 \leq 0.086 \leq 0.102$	$0.127 \leq 0.188 \leq 0.264$	$0.783 \leq 0.869 \leq 0.947$
250:350	$0.188 \leq 0.221 \leq 0.256$	$0.077 \leq 0.116 \leq 0.161$	$0.886 \leq 0.930 \leq 0.975$
350:450	$0.190 \leq 0.241 \leq 0.304$	$0.009 \leq 0.016 \leq 0.048$	$0.929 \leq 0.965 \leq 0.985$

V. Conclusion

We presented a computationally inexpensive range-dependent two-state model that allows to accurately reproduce the effects of realistic channel conditions on the I2V link. Parameters of our model have been estimated using an extensive set of measurement data for 78 different granularities in range $\{30, 40, \ldots, 800\}\,\mathrm{m}$. Comparing burst and gap length distributions, as well as FSR and the main performance indicators of the measured and the modeled sequences, we conclude that the overall error statistics of the measurement can be closely approximated by the model with all granularities of considered range. However in order to precisely model realistic channel effects that have straightforward influence on such significant performance indicator as reliable communication range, use of smaller granularities for modeling is advisable. Finally, we provide a complete set of model parameters for granularity of $100\,\mathrm{m}$. This set of parameters can be directly used as an input to a HMM generation algorithm in order to obtain realistic error patterns.

References

[1] J. Otto, F. Bustamante, and R. Berry, "Down the Block and Around the Corner The Impact of Radio Propagation on Inter-vehicle Wireless Communication," in *29th IEEE International Conference on Distributed Computing Systems, 2009*, June 2009, pp. 605 –614.

[2] E. Giordano, R. Frank, A. Ghosh, G. Pau, and M. Gerla, "Two Ray or not Two Ray this is the price to pay," in *6th IEEE International Conference on Mobile Adhoc and Sensor Systems, 2009*, October 2009, pp. 603 –608.

[3] J. Karedal, F. Tufvesson, T. Abbas, O. Klemp, A. Paier, L. Bernado, and A. Molisch, "Radio Channel Measurements at Street Intersections for Vehicle-to-Vehicle Safety Applications," in *71st IEEE Vehicular Technology Conference, 2010*, May 2010.

[4] A. Paier, J. Karedal, N. Czink, H. Hofstetter, C. Dumard, T. Zemen, F. Tufvesson, C. Mecklenbrauker, and A. Molisch, "First Results from Car-to-Car and Car-to-Infrastructure Radio Channel Measurements at 5.2 GHZ," in *18th IEEE International Symposium on Personal, Indoor and Mobile Radio Communications, 2007*, September 2007.

[5] J. Maurer, T. Fugen, and W. Wiesbeck, "Narrow-band Measurement and Analysis of the Inter-Vehicle Transmission Channel at 5.2 GHz," in *55th IEEE Vehicular Technology Conference, 2002*, vol. 3, 2002, pp. 1274 – 1278.

[6] J. Maurer, T. Fugen, T. Schafer, and W. Wiesbeck, "A new Inter-Vehicle Communications (IVC) Channel Model," in *60th IEEE Vehicular Technology Conference, 2004*, vol. 1, September 2004, pp. 9 – 13.

[7] A. Schmitz and M. Wenig, "The Effect of the Radio Wave Propagation Model in Mobile Ad hoc Networks," in *9th ACM International Symposium on Modeling Analysis and Simulation of Wireless and Mobile Systems, 2006*. ACM, 2006, pp. 61–67.

[8] I. Stepanov and K. Rothermel, "On the Impact of a more Realistic Physical Layer on MANET Simulations Results," *Ad Hoc Networks*, vol. 6, no. 1, pp. 61–78, 2008.

[9] J. Mittag, S. Papanastasiou, H. Hartenstein, and E. Ström, "Enabling Accurate Cross-Layer PHY/MAC/NET Simulation Studies of Vehicular Communication Networks," *Proceedings of the IEEE*, vol. 99, no. 7, pp. 1311 –1326, July 2011.

[10] http://www.cvisproject.org.

[11] E. N. Gilbert, "Capacity of a burst-noise Channel," *Bell System Technical Journal*, vol. 39, no. 9, pp. 1253–1265, 1960.

[12] L. E. Baum, T. Petrie, G. Soules, and N. Weiss, "A Maximization Technique Occurring in the Statistical Analysis of Probabilistic Functions of Markov Chains," *The Annals of Mathematical Statistics*, pp. 164–171, 1970.

[13] W. Feller, *An Introduction to Probability Theory and its Applications*. John Wiley & Sons, 2008, vol. 2.

[14] J. Gozalvez, M. Sepulcre, and R. Bauza, "IEEE 802.11 p vehicle to infrastructure communications in urban environments," *Communications Magazine, IEEE*, vol. 50, no. 5, 2012.